Journal of Experimental Botany
doi:10.1093/jxb/erx249

RESEARCH PAPER

Crop-model assisted phenomics and genome-wide association study for climate adaptation of *indica* rice. 1. Phenology

Michael Dingkuhn[1,*], Richard Pasco[2], Julie Pasuquin[2], Jean Damo[2], Jean-Christophe Soulié[1], Louis-Marie Raboin[1], Julie Dusserre[1], Abdoulaye Sow[3], Baboucarr Manneh[3], Suchit Shrestha[2], Alpha Balde[3] and Tobias Kretzschmar[2]

[1] Cirad, Umr AGAP (Dept BIOS) and Upr AIDA (Dept ES), F-34398, Montpellier, France
[2] IRRI, CESD Division, DAPO Box 7777, Metro Manila, Philippines
[3] Africa Rice Center, Sahel Station, PB 96, St Louis, Senegal

* Correspondence: michael.dingkuhn@cirad.fr

Received 14 February 2017; Editorial decision 20 June 2017; Accepted 27 June 2017

Editor: Greg Rebetzke, CSIRO Agriculture and Food

Abstract

Phenology and time of flowering are crucial determinants of rice adaptation to climate variation. A previous study characterized flowering responses of 203 diverse *indica* rices (the ORYTAGE panel) to ten environments in Senegal (six sowing dates) and Madagascar (two years and two altitudes) under irrigation in the field. This study used the physiological phenology model RIDEV V2 to heuristically estimate component traits of flowering such as cardinal temperatures (base temperature (T_{base}) and optimum temperature), basic vegetative phase, photoperiod sensitivity and cold acclimation, and to conduct a genome-wide association study for these traits using 16 232 anonymous single-nucleotide polymorphism (SNP) markers. The RIDEV model after genotypic parameter optimization explained 96% of variation in time to flowering for Senegal alone and 91% for Senegal and Madagascar combined. The latter was improved to 94% by including an acclimation parameter reducing T_{base} when the crop experienced low temperatures during early vegetative development. Eighteen significant ($P<1.0 \times 10^{-5}$) quantitative trait loci (QTLs) were identified, namely ten for RIDEV parameters and eight for climatic index variables (difference in time to flowering between key environments). Co-localization of QTLs for different traits were rare. RIDEV parameters gave QTLs that were mostly more significant and distinct from QTLs for index variables. Candidate genes were investigated within the estimated 50% linkage disequilibrium regions of 39 kB. In addition to several known flowering network genes, they included genes related to thermal stress adaptation and epigenetic control mechanisms. The peak SNP for a QTL for the crop parameter *Tbase* ($P=2.0 \times 10^{-7}$) was located within *HD3a*, a florigen that was recently identified as implicated in flowering under cool conditions.

Key words: Candidate genes, cold tolerance, flowering, HD3a florigen, heuristics, *Oryza sativa* L., photoperiod sensitivity, RIDEV crop model.

Introduction

Phenology, in terms of plant developmental processes that govern organ production and flowering time, is of foremost importance to crop adaptation (Dingkuhn, 1995; Fukai, 1999; Shrestha *et al.*, 2013). A precursor study (Dingkuhn *et al.*, 2015*b*) characterized environment-driven variation and genetic diversity of time to flowering in ten environments

in Senegal and Madagascar for an irrigated rice diversity panel of 203 accessions (the ORYTAGE *indica* subset; Cirad ORYTAGE project and GRiSP Global Rice Phenotyping Network, http://ricephenonetwork.irri.org), consisting of landraces and improved varieties. It was characterized for genotypic diversity and plasticity of phenology as challenged by day length, temperature, and altitude. This study carries the analysis two steps further by (i) using a physiological model (RIDEV) to extract physiological trait information from the dataset using heuristics (Hammer *et al.*, 2002; Rebolledo *et al.*, 2015) and (ii) conducting a genome-wide association study (GWAS) that relates single nucleotide polymorphisms (SNPs) to the variation of the traits.

Although measuring time to flowering is easy, it is difficult to dissect the various traits contributing to its variability, particularly if the objective is not only to predict flowering (as needed by agronomists; Dingkuhn, 1995) but also to obtain traits that correlate with genetic control mechanisms (needed by geneticists and breeders). As a precursor to the present approach, Dingkuhn and Miezan (1995) used RIDEV to dissect day length and thermal response parameters of flowering for 50 rice varieties grown at ten sowing dates in Senegal. For this study, we developed RIDEV V2, incorporating novel findings on crop microclimate (Julia and Dingkuhn, 2012, 2013) and photoperiod response (Dingkuhn *et al.*, 2008). We apply it to dissect flowering responses of the ORYTAGE *indica* panel to ten environments differing in season, latitude and altitude, and consequently in climate and day length.

The underlying assumption of any heuristic phenotyping approach is that crop model parameters share similarity with genetic parameters controlling the traits, resulting in correlations between genotypic parameter variation and specific DNA polymorphisms. RIDEV, like many phenology models, assumes flowering responses to consist of genotype-specific thermal-time budgets (constitutive trait) and day length and temperature responses (inducible), the latter depending on constitutive cardinal temperatures. This simple model stands in contrast to the complexity of gene networks controlling flowering in rice (Shrestha *et al.*, 2014). At least 19 network genes participate in two parallel but interconnected pathways, at the bottom of which are *HD3a* (promoting flowering under short days) and *RFT1* (long days). While several of the network genes are under the control of the circadian clock, others are connected to genes conveying thermal and stress effects, such as *Ghd7*, which retards flowering under low temperatures by suppressing the long-day flowering stimulus (Ehd1→RFT1 pathway; Song *et al.*, 2012). Day length, temperature and stress signaling are thus connected, and the more variable the environment, the more network genes participate in flowering control.

This study aims to better understand environmental and genetic control of *indica* rice phenology in photo-thermally variable tropical environments. The specific objectives were to (i) develop a modeling approach to extract functional component traits from flowering data; (ii) conduct GWAS on estimated model parameters and compare their performance with those of simpler climatic index variables; and (iii) identify candidate genes and DNA polymorphisms putatively involved in climatic adaptation of flowering.

Materials and methods

Experimental design

This study used data from experiments in Senegal and Madagascar presented in detail by Dingkuhn *et al.* (2015*a*,*b*). Only essential information is reported here.

Senegal

The experiment was conducted at the AfricaRice Sahel Station at Ndiaye, Senegal (16°12′N, 16°16′W, 8 m above sea level; asl). It used an augmented design with six blocks and two factors (sowing date, genotype). Each block had six sowing dates and 38 genotypes plus four replicated checks (IR64, Sahel 108, N22, Chomrong). Subplots were 1 m×1 m and pre-germinated seed was hill-wise dibbled onto wet puddled soil at 20 cm×20 cm. Fields were kept flooded at 5–10 cm depth throughout. Fertilizer inputs were 120–60–60 (N–P–K, kg ha^{-1}). Weeds were controlled by hand and birds with nylon fishnets. The soil was a heavy, slightly acid, vertisol clay.

Sowing dates were 7 February, 7 March and 7 April (hot-dry season), 17 July (wet season), 17 September (cool during late-season), and 19 October (cool-dry season) 2009. Days to 50% flowering were determined when half of the panicles at the center of the subplot were shedding pollen. Weather was recorded with a HOBO U30-NRC weather station (Onset Corp., Bourne, MA, USA) located on-farm.

Madagascar

Experimental sites were Ambohitromby (Hautes Terres, Région d'Antsirabe, 19°52′S, 46°59′E, 1494 m asl) and Ivory (19°32′S, 46°24′E, 869 m asl). The experiment, identical at both sites, was a randomized complete-block design with three replications. Elemental plots (variety) were 0.6 m×1.4 m (3 × 7 hills planted at 20 cm×20 cm, with the central row used for observations). Pre-germinated seed was sown on 3 December 2009 and 6 December 2010 at Ivory and on 11 December 2009 and 15 December 2010 at Ambohitromby in a seedling nursery and transplanted 15–20 d after sowing. Plots were kept flooded at 5–10 cm throughout. Fertilizer was green manure (5 t ha^{-1}) and 81–27–49 (N–P–K, kg ha^{-1}). Weeding was manual and fungicide treatment followed the local standard. The soil was acid (pH 4.5) at both locations, with clay texture at Ambohitromby and clay loam at Ivory.

Observations of flowering were performed as in Senegal but on the five central plants on the middle row of the plots. Check varieties were as in Senegal but cv. Chomrong was absent.

Weather was monitored daily with ENERCO 404 Series (CIMEL Electronique, Paris, France) automatic weather stations located on-farm.

Germplasm

A subsample of 203 *indica* accessions from the ORYTAGE species-wide (*O. sativa* L.) diversity panel of Cirad (http://ricephenonetwork.irri.org/diversity-panels/orytage-diversity-panels) was investigated. The population covered improved and traditional varieties from all tropical regions but had large subsets from Madagascar (34) and W. Africa (44, of which 30 were improved lines from AfricaRice bred in Senegal). Twenty improved varieties and lines were from IRRI (Philippines). A complete list of the accessions' geographical origin and seed sources is presented in Supplementary Table S1 at *JXB* online.

Genotyping by sequencing

Genotyping was conducted at Diversity Arrays Technology Pty Ltd (Australia) using genotyping by sequencing (GBS) previously described by Courtois *et al.* (2013). A combination of *Pst*I–*Taq*I restriction enzymes was used to reduce genome complexity. Sequences

were trimmed at 69 bp (5 bp of the restriction fragment plus 64 bases, with a minimum quality score of 10). An analytical pipeline developed by DArT P/L was used to produce DArT score tables (corresponding to the presence/absence of any given sequence) and tables of SNPs within the 69 bp sequences. Both DArT and SNP markers were used. DArT markers correspond to a change in the 5 bp restriction site: it can be an SNP at any of the five positions or an indel. Since the lines were homozygous, the fact that DArT are dominant markers did not matter. The positions of the markers on the Nipponbare sequence were determined by aligning the sequences to the Os-Nipponbare-Reference-IRGSP-1.0 pseudomolecule assembly (Kawahara *et al.*, 2013). Markers that had no or several positions on the Nipponbare sequence, more than 15% missing data, or a minor allele frequency below 3% were discarded. Heterozygotes were treated as missing data. Missing data were imputed using Beagle v3.3.2 (Browning and Browning, 2007). Beagle infers the haplotype phase and missing data on a chromosome basis using an empirical, localized haplotype-cluster model that adapts to local linkage disequilibrium (LD) by an iterative expectation-maximization algorithm.

Genomics data resource used for association mapping

Data cleaning involved removing sequences having more than one hit on the pseudomolecules, which were discarded, as well as markers with call rates below 80% or having minor allele frequency below 2.5%. After data cleaning and before imputation of the GBS resource, the rate of missing data was 6.5%. The final dataset was composed of 16 232 markers (8214 DArT and 8018 SNP markers), which corresponded to a density of one marker per 24 kb. There were nine gaps of more than 500 kb devoid of markers on chromosomes 2, 4, 6, 7, 8, and 11, of which two were about 1 Mb.

Association mapping

GWAS was conducted for each trait using a mixed model with control of the structure and kinship under Tassel v5.0 (Bradbury *et al.*, 2007). The threshold to declare an association highly significant was set at a probability level of $P<1 \times 10^{-5}$. In addition associations having $1 \times 10^{-5}<P<1 \times 10^{-4}$ are presented in the Supplementary Table S3. The 50% decay genomic distance of LD was calculated according to Sved (1971) (see Supplementary Fig. S5). Supporting SNPs, as a supplemental measure to evaluate a QTL, were defined as SNPs with $P<1 \times 10^{-3}$ located within ±LD. Quantile–quantile plots are presented in Supplementary Fig. S1.

RIDEV V2 model

General

The RIDEV V2 model is an improved version of RIDEV described and validated by Dingkuhn *et al.* (1995), Dingkuhn and Miezan (1995), and Dingkuhn (1995, 1997), and later described as an agronomic decision tool by Wopereis *et al.* (2003). It simulates the duration of phenological phases, the timing of panicle initiation (PI) and flowering (FL) events, and the incidence of cold- or heat-induced sterility. RIDEV V2 can be used in simulation mode (phenology/sterility prediction) or heuristic (reverse) mode to estimate genotypic parameters. The main improvements in RIDEV V2 are (i) the use of the *Impatience* model of day length effects on PI (Dingkuhn *et al.*, 2008); (ii) improved simulation of floodwater temperature as a function of estimated leaf area index (LAI) dynamics and weather variables; (iii) simulation of air humidity (RH) and air temperature (T_a) effect on time of day of anthesis (TOA; Julia and Dingkuhn, 2012); and (iv) simulation of panicle temperature at TOA as a function of T_a, RH, wind speed and solar radiation (R_s) (Julia and Dingkuhn, 2013). A schematic diagram of RIDEV V2 is shown in Fig. 1. Detailed description and manual are provided in http://umr-agap.cirad.fr/en/equipes-scientifiques/plasticite-phenotypique-et-adaptation-des-monocotyledones/principaux-resultats/ridev. Source code is provided in Supplementary Protocol S1.

RIDEV V2 operates deterministically at daily time steps, with hourly loops used to calculate thermal time and TOA. The model is implemented in the C++ language and coupled with routines in *R*

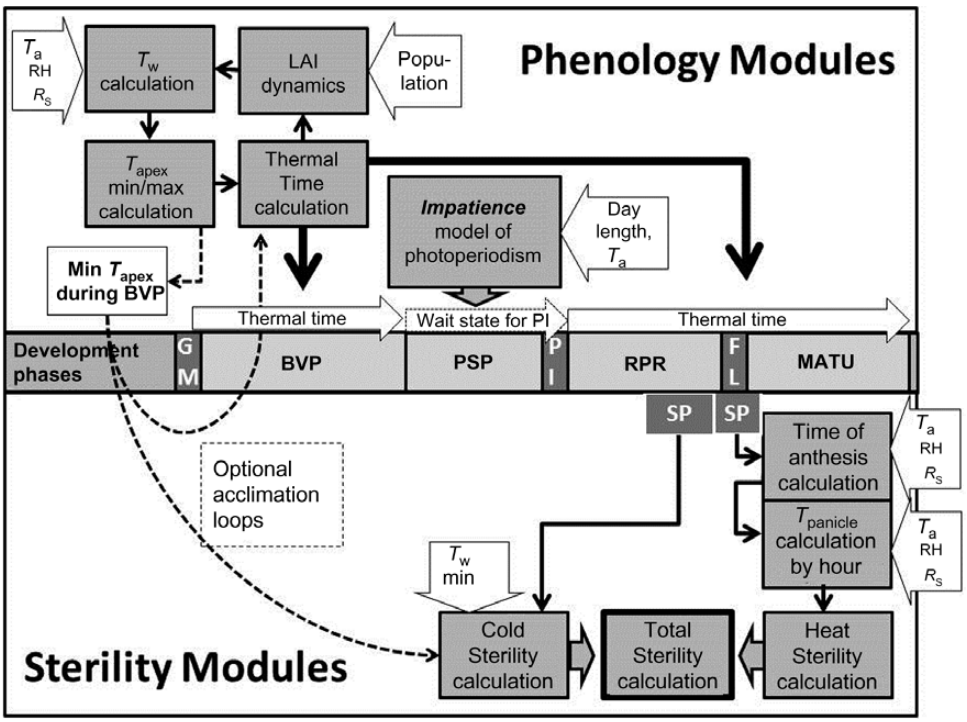

Fig. 1. Schematic diagram of RIDEV V2 model. Only the phenology modules (top) were used in this study. Dark gray boxes are modules, white boxes are input data, black arrows are data flow, and white arrows are phenological progress. BVP, basic vegetative phase; FL, flowering; GM, germination; MATU, maturation phase; PI, panicle initiation; PSP, photoperiod-sensitive phase; RH, air humidity; RPR, reproductive phase; R_s, solar radiation; SP, stress sensitive phase; T_a, air temperature; T_{apex}, shoot apex temperature; T_w, water temperature.

for R-Genoud parameter estimation procedures (refer to website). The user has a choice of which crop parameters to optimize within user-set value ranges, and which parameters to freeze at a user-defined value. Input data are read from and results written into text files. Input and output variables used here are presented in Table 1 (complete list in Supplementary Table S2). We describe only phenology modules used here.

Phenological phases

The model simulates crop development from sowing until physiological maturity, with crop establishment included in the basic vegetative phase (BVP). No time was allocated to seedling emergence as pre-germinated seed was sown directly onto moist soil. The BVP is followed by a photoperiod sensitive phase (PSP) ending with PI, then a reproductive phase (RPR) ending with FL and a maturation phase (MATU). Each phase except PSP has a genotype-specific thermal-time budget (*BVPsum*, *RPRsum*, *MATUsum*). *RPRsum* was considered as constant (400 °C d) because it is known to vary less than BVP among genotypes (although this is poorly documented). MATU was not studied here. The duration of PSP depends on day length and temperature (see below).

Thermal time and cardinal temperatures

Development proceeds in thermal-time increments, calculated with genotypic cardinal temperatures *Tbase* and *Topt* (Dingkuhn and Miezan, 1995). Linear development response between *Tbase* and *Topt* is assumed. This may be inaccurate for temperatures near *Tbase* but was considered acceptable as we were seeking genotypic differences and not necessarily absolutes. For each day, a physiological heat value (*Tphys*, state variable) is calculated by estimating it on an hourly basis and averaging it for the 24 h of day(i):

$$Tphys(i) = \text{average}\left[\min(Tact, Topt) - Tbase\right](i)$$

Daily *Tphys* is accrued until *SumTPhys* attains the genotypic target for the current phenological phase (e.g. *BVPsum* for BVP). Hourly temperatures are estimated from daily $T_{a(min)}$, $T_{a(max)}$ (at 2 m) and astronomic day/night length using a standard diurnal temperature pattern (similar to Reicosky *et al.*, 1989; details on website). This procedure is applied identically to T_{min} and T_{max} for air, water, shoot apex or panicle.

Photoperiod sensitivity

The *Impatience* model described and validated by Dingkuhn *et al.* (2008) was chosen among several other options provided in RIDEV. *Impatience* is based on a threshold photoperiod for floral induction, with a mechanism causing gradual threshold lowering (longer days enable induction) as the wait-state for the signal is prolonged ('impatience'). This model simulated best the flowering observed for some highly day length sensitive rices (Dingkuhn *et al.*, 2015*b*) and sorghums (Dingkuhn *et al.*, 2008). Parameters *PPcrit* and *PPsens* were fitted by optimization.

Water temperature

The shoot apex of irrigated rice is submerged until stem elongation. Water temperature (T_w) deviates from T_a depending on ground cover, time of day and weather (Dingkuhn *et al.*, 1995). In RIDEV, daily $T_{w(min)}$ and $T_{w(max)}$ are calculated from canopy light transmission ratio (LTR, obtained from LAI using Lambert–Beer's law) and $T_{a(min)}$ and $T_{a(max)}$ using empirical functions obtained from *ca*. 5000 measurements in diverse climatic situations (Julia and Dingkuhn, 2012, 2013). Simulated and observed data from that source are compared in Supplementary Fig. S2. As climatic inputs, only T_a is used in order to limit data requirements. A proxy for RH and R_s is used in the form of $[T_{a(max)} - T_{a(min)}]$, as high diurnal amplitudes are associated with low RH and high R_s. Equations 1 and 2 were used to calculate water temperature (T_w):

$$T_{w(min)} = T_{a(min)} + a(T_{a(max)} - T_{a(min)}) \times (1 - \text{LTR}) + b(T_{a(max)} - T_{a(min)}) \times \text{LTR} + c((T_{a(max)} - T_{a(min)})\text{^}1.2) \quad (1)$$

with a=0.658; b=0.425; c=−0.303.

$$T_{w(max)} = T_{a(max)} + [a(T_{a(max)} - T_{a(min)}) \times (1 - \text{LTR}) + b(T_{a(max)} - T_{a(min)}) \times \text{LTR}] \times (T_{a(max)} + c)/20 \quad (2)$$

with a=−0.728; b=0.275; c=−18.46, where T_a is air temperature at 2 m in the field.

Table 1. *RIDEV V2 parameters and input/output variables used in this study*

X ... *Y* denotes biologically reasonable ranges.

Parameter/variable	Definition
Scenario parameters	
Latitude	xx.yy, decimal (degrees)
SowingDate	dd/mm/yyyy
Transplanting	0 or 1, binary
DDTransplantingShock	0 ... 200 (default=100), development lag in thermal time units (°C d)
POP	Plant population density, 50 000 ... 1 000 000 (plants ha^{-1})
Input variables (variables in brackets only needed for heat sterility under flooded cultivation)	
Tmin	Daily minimum air temperature at 2 m (°C)
Tmax	Daily maximum air temperature at 2 m (°C)
Crop parameters for phenology (can be optimized by R-Genoud; refer to Table 2)	
Tbase	Base temperature, 0 ... 15 (°C)
Topt	Optimum temperature, 20 ... 40 (default=30) (°C)
BVPsum	duration of BVP, 200 ... 1000 (°C d)
PPcrit	Critical day length above which flowering is delayed, 11 ... 12 (h)
PPsens	Sensitivity of photoperiod response, 0.4 (sensitive) ... 2.0 (insensitive) (unitless)
AcclimTb	Acclimation effect of low *T* (initial 30 d after sowing) on *Tbase*, 0 ... 2
Output variables	
DSowFlowering	Time sowing to flowering (d)

This model was validated with independent field observations at the Ndiaye and Fanaye sites of AfricaRice Center in Senegal (Fig. 2), resulting in a $T_{w(sim)}$ *vs* $T_{w(obs)}$ correlation with R^2=0.87. In this figure, observed T_a is also plotted against observed T_w as small dots. Their strong deviation from the 1:1 line by up to 10 °C indicates that the model predicting T_w was necessary. A separate experimental validation of Eq. 1 predicting $T_{w(min)}$ was presented by Dingkuhn *et al.* (2015*b*).

Apex temperature

Since the shoot apex is under the water line during much of the crop cycle, apex temperature (T_{apex}) was considered to be equal to T_w, except during RPR, during which internode elongation lifts the apex towards the canopy top. We therefore simulated T_{apex} to linearly converge with T_a in the course of RPR.

Transplanting shock

RIDEV phenology takes into account development delays during BVP caused by transplanting, which is usually about 1 week, depending on practices. For the Madagascar experiments, which were transplanted, a lag of 100 °C d was assumed for BVP for all genotypes.

Acclimation to cold conditions

Parameter estimation mostly provided accurate flowering predictions across the ten environments (six in Senegal and four in Madagascar), but not for some genotypes. We hypothesized that this was caused by cold acclimation at high altitude in Madagascar whereas in Senegal, periods with cold nights were short and strictly seasonal (Dingkuhn *et al.*, 2015*b*). A function was implemented in RIDEV reducing base temperature (T_{base}) linearly as mean $T_{a(min)}$ during the initial 30 d after sowing dropped below 18 °C, as follows:

$$TbaseCor = Tbase - AcclimTb \times \max\left[0,(18 - AvTmin30d)\right]$$

where *TbaseCor* is the acclimated *Tbase* applied for the rest of the crop cycle, and

AvTmin30d is the average $T_{a(min)}$ observed during the initial 30 d after sowing.

The critical $T_{a(min)}$ of 18 °C for acclimation was chosen because chilling stress was observed in *indica* rice below it (Dingkuhn *et al.*, 1995). The underlying hypothesis was that acclimation for reproductive stages happens during early vegetative stages, arbitrarily set to 30 d. The crop coefficient *AcclimTb* attenuates the acclimation response and was optimized along with the other parameters. At *AcclimTb*=0 no acclimation happens.

RIDEV parameters used in the study

Table 1 presents RIDEV V2 parameters used (a complete list of parameters/variables is given in Supplementary Table S2). Only $T_{a(min)}$ and $T_{a(max)}$ were used as climatic input. For Senegal, *Transplanting* was 0 and in Madagascar it was 1. Plant population *POP* was 600 000 ha^{-1} in Senegal and 250 000 in Madagascar. Whenever crop parameter *Topt* was not estimated, it was set to default=30 °C. Ripening phase *RPRsum* was set to 400 °C. As output, only the duration from sowing to flowering was used.

Choices of parameters and ranges for estimation

Parameters were either fixed to default values or optimized by R-Genoud within physiologically relevant ranges, whereby the parameters were co-optimized in one procedure. The accuracy of model prediction of observed days from sowing to flowering across the ten environments was evaluated by the normalized least-square error method (cost function). R-Genoud varied parameter values by genetic algorithm until the cost function was minimized, involving 10^6–10^7 simulations per run. Four estimation runs are reported here (Table 2), one of which (Run2) included only Senegal data and excluded *Topt* from parameter optimization. Limiting the number of parameters improved GWAS associations while degrading phenotype predictions. When parameter number was too small (Run0), both GWAS and phenotype prediction were poor. Run3 made use of the acclimation function to low temperatures.

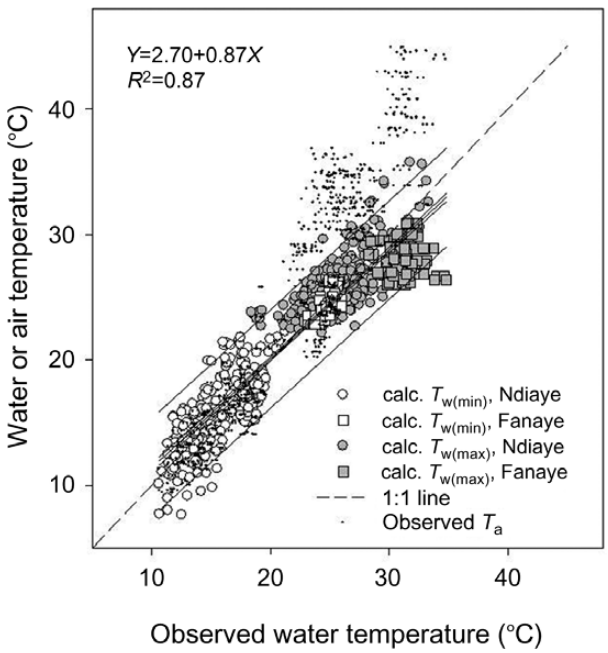

Fig. 2. Validation of RIDEV V2 calculation of water temperature using independent data (courtesy of Africa Rice Center). The correlation between calculated and observed minimum and maximum water temperature (T_w) is shown across all rice developmental stages, two sites and three plant population densities or continuously flooded Sahel 108 rice. Observed periods were 15 February to 28 May 2012 at Fanaye (hot-dry season, inland) and 6 October 2012–4 March 2013 at Ndiaye (cool-dry season, coastal) in the Senegal river valley. Small dots are observed air temperature, indicating a large air–water differential that was explained by the model. The 95% confidence interval (close to regression line) and the prediction interval (parallel straight lines) are provided.

Traits analysed by GWAS

Two types of traits were analysed, (i) index variables directly calculated from flowering dates and (ii) RIDEV parameters. The index variables were described by Dingkuhn *et al.* (2015*b*) and are summarized as follows.

BVPindex (d)

BVPindex, estimating BVP, represented the shortest time from sowing to PI observed among the 6 sowing dates in Senegal, with PI estimated at 25 d before flowering (De Datta, 1981). This occurred on sowings in July or September when photoperiod effects were smallest, and we assumed PSP to be nil. *BVPindex* varied between 20 and 80 d.

PPindex (d)

Sowing in Senegal in February, March and April increased duration from sowing to flowering in photoperiod-sensitive genotypes (Dingkuhn and Miezan, 1995; for theory refer to Dingkuhn *et al.*, 2008). For sowing in February, interactions with low $T_{a(min)}$ were likely. (The 'hot-dry season' is cool at the onset.) To avoid this we used the difference in duration between March (strong photoperiod signal) and July (weak) sowings as an index for photoperiod sensitivity.

Table 2. *RIDEV parameter estimation runs using R-Genoud*

Data sets for Senegal included six environments (six sowing dates) and for Madagascar four environments (2 altitudes×2 years). Fields marked × indicate inclusion in estimation run.

Estimation run	Data sets included		Crop parameters estimated						Figures
	Senegal	Madagascar	*Tbase*	*Topt*	*BVPsum*	*PPcrit*	*PPsens*	*AcclimTb*	
0	×	×	Set to 12	Set to 30	×	Set to 11.5	×	Set to 0	—
1	×	×	×	×	×	×	×	Set to 0	4A, B, 5B, 6B, C, 8B, C
2	×	Not used	×	Set to 30	×	×	×	Set to 0	7B
3	×	×	×	×	×	×	×	×	4C, 7C

COLDindex (dimensionless)
For sowing in mid-July and October in Senegal, day length effects are negligible (Dingkuhn *et al.*, 1995) but the October crop is exposed to low $T_{a(min)}$ during RPR, causing delayed flowering. We used the ratio October/July duration to flowering as an index of sensitivity to cold. A ratio (instead of difference) was used because temperature presumably affects duration cumulatively throughout development.

ALTindex (d)
The difference in duration to flowering between the high-altitude site in Madagascar and the warm, sea-level environment in Senegal for the crop sown in July was used as an index for the altitude effect, which is possibly but not necessarily thermal.

RIDEV parameters *Tbase*, *Topt*, *BVPsum*, *PPsens* and *AcclimTb* were also used. For *PPsens*, the reciprocal value gave the best results (1/*PPsens*). In addition, the derived parameter *BVPmin* was used. It was calculated as [*BVPmin*=*BVPsum*/(*Topt*−*Tbase*)] and expresses the shortest possible time in days for a genotype to attain PI. Estimation of *PPcrit* helped improving phenotype prediction but gave no significant GWAS peaks, and *PPsens* peaks were little affected by *PPcrit* estimation.

Searches for annotated genes within QTLs

Annotated genes within ±100 kB of a given SNP were extracted from Phytozome (Joint Genome Institute (JGI), https://phytozome.jgi.doe.gov) and MSU database (Michigan SU, http://rice.plantbiology.msu.edu/). Further functional and expression-related information was extracted from databases GeneVisible (https://genevisible.com/), PlaNet (http://aranet.mpimp-golm.mpg.de/), Gramene (http://archive.gramene.org/), UniProt (http://www.uniprot.org/), RiceXPro (http://ricexpro.dna.affrc.go.jp/), RiceChip (http://www.ricechip.org/) and gabi (https://www.gabipd.org/).

Statistics

Linear regression analyses and frequency distributions were conducted with SigmaPlot 12.3 (Systat Software Inc.).

Results

Sensitivity of simulation outcome to RIDEV crop parameters

A sensitivity analysis was conducted for RIDEV parameter effects on time to flowering for four contrasting environments (Supplementary Fig. S3). Parameters *Tbase*, *Topt* and *BVPsum* contributing to thermal response showed similar patterns across those environments but differed in slope and curvature of the response. For this reason, the parameter *BVPmin* was calculated, integrating effects of the three parameters. By contrast, the environments distinguished strongly among effects of *PPsens*, *AcclimTb* and the three temperature-related parameters. *Tbase*, *Topt* and *BVPsum* were retained for GWAS analysis, however, because each gave more and functionally plausible genomic associations than the aggregated parameter *BVPmin* (refer to sections below).

Estimated RIDEV model parameters

RIDEV parameters were estimated for each accession across environments (Table 2). Frequency distributions for estimation Run1 and Run3 are presented in Fig. 3 for the parameters. *Tbase* was normally distributed for Run1 with a mean at about 5.5 °C (Fig. 3A). This value is low as compared with those reported for rice, mostly superior to 10 °C (Dingkuhn and Miezan, 1995). When *Tbase* was estimated for Senegal data only (Run2, histogram not presented), however, mean *Tbase* was 11.5 ± 2.6 (SD) °C. Inclusion of higher altitude Madagascar data with continuously low night temperatures thus reduced *Tbase*, indicating acclimation. Inclusion in RIDEV of acclimation (Run3) resulted in 9.4 ± 4.1 °C mean *Tbase* (Fig. 3A, histogram). Acclimation thus explained much of the difference in *Tbase* estimation for Senegal *vs* Senegal and Madagascar combined.

Estimated *Topt* varied widely between 20 and 35 °C (Fig. 3B) and was similar for Run1 and Run3. (The temperature window for *Topt* estimation was capped at 35 °C because higher temperatures occurred rarely, potentially causing meaningless parameter estimations outside the conditions encountered. *Topt* values above the observed range do not affect simulations but would increase noise in GWAS.)

Estimated 1/*PPsens* (Fig. 3C) was <1.5 for most accessions, indicating photoperiod insensitivity, but the distribution showed a protracted tail towards higher values, indicating delayed flowering under long days. Distributions were similar for Run1 and Run3.

Parameter *BVPmin* (Fig. 3D) was normally distributed, with a mean of about 50 d (Run1) and a range between 20 and 80 d. The distribution reflected the strong representation of short to medium-duration materials maturing at 100–120 d after sowing (data not presented), with a BVP of 40–60 d. Run3 reduced *BVPmin* by about 10 d because the additional parameter

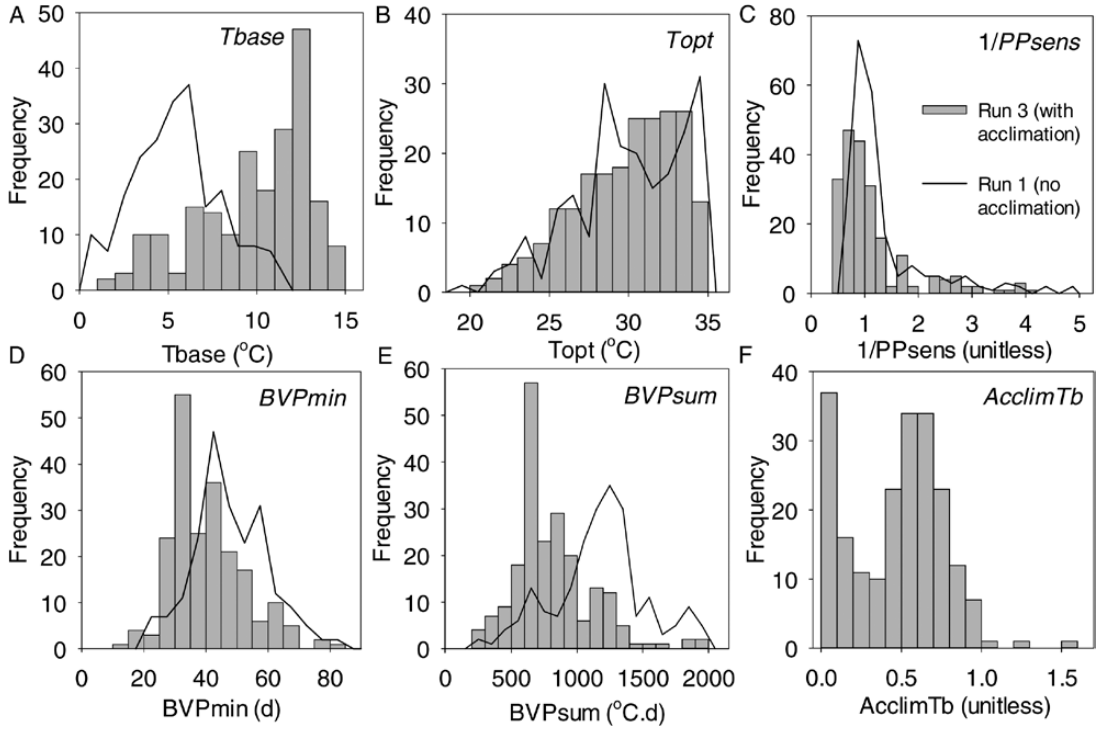

Fig. 3. Frequency distributions (number of accessions per class) of estimated RIDEV V2 parameter values for Senegal and Madagascar environments combined, for Run1 (no cold acclimation considered) and Run3 (parameter *AcclimTb* co-optimized). Run1 and Run3 gave similar distributions for *Topt* (B), 1/*PPsens* (C) and *BVPmin* (D). Co-optmization of *AcclimTb* gave more realistic values for *Tbase* (A; higher), which necessarily caused lower values for *BVPsum* (E). (For frequency distributions for index variables refer to Supplementary Fig. S4n.)

AcclimTb helped explaining better the earliest observed flowering for many accessions. *BVPsum* (Fig. 3E; corresponding to *BVPmin* but expressed in thermal time) decreased for Run3 *vs* Run1, which was an expected result of higher *Tbase* estimations. *AcclimTb* (Fig. 3F), only estimated in Run3, was bimodally distributed, indicating a subpopulation that acclimatized little (*AcclimTb*<0.3) and another that acclimatized strongly.

Phenotypic variation of index variables was reported by Dingkuhn *et al.* (2015*b*). For their frequency distribution refer to Supplementary Fig. S4.

Variation in time to flowering explained by the model

When only two parameters were estimated (*BVPsum*, *PPsens*; Table 2: Run0), the model explained only 76% of variation of time to flowering (Fig. 4A; same data used for parameterization and simulation). With the inclusion of estimated cardinal temperatures (Run1, Fig. 4C), the correlation increased to R^2=0.91, indicating that the thermal response parameters were needed. The case of the mildly photoperiod-sensitive check Sahel 108 is given in Fig. 4B (R^2=0.92), where duration varied between 65 and 120 d. Duration was longer for Madagascar than Senegal due to cooler climate, but variation was observed within both countries due to altitude (Madagascar) or sowing date (Senegal).

Across all accessions, the correlation between simulated and observed duration to flowering was much stronger for Senegal environments alone (Fig. 4D, Run2: R^2=0.96) than for all environments combined (Fig. 4C, Run1: R^2=0.91), owing to cases wrongly predicted for Madagascar. Observed and simulated durations were between 50 and nearly 250 d and inaccurate simulations occurred mostly in the middle range. Since simulated cases deviating by >10 d from observation represented less than 1% of all cases generally concerned only one environment for any given accession, Run1 parameter estimations were accepted and used for GWAS.

A marked improvement of the simulated *vs* observed correlation was achieved with the implementation of the cold-acclimation hypothesis (Run3), which reduced *Tbase* when the crop experienced cool conditions during the initial 30 d (Fig. 4E; R^2=0.94). Most of the apparent outliers observed in Fig. 4D disappeared when acclimation was considered, indicating that they were not random errors.

Genomic associations for photoperiod sensitivity

GWAS results for *PPindex* are shown in Fig. 5A. Four QTLs were detected, located on chr1 (*P1(1)i*), chr6 (*P6i*), chr7 (*P7i*) and chr11 (*P11(2)i*). Their *P*-values were between 1.0×10^{-5} and 2.5×10^{-6}, and each QTL had several supporting SNPs (Table 3).

The model parameter 1/PPsens gave the same QTLs for estimation Run0 (Table 2: only two parameters estimated) and Run1 that had cardinal temperatures co-estimated. We will henceforth refer to the results of Run1.

Among the four QTLs detected for *PPindex*, none was detected for corresponding model parameter *1/PPsens*. However, two were physically close, with 497 kb separating *P6m* from *P6i* and 709 kb separating *P11(3)m* from *P11(2)i* (Table 3). In both cases, *1/PPsens* gave more significant

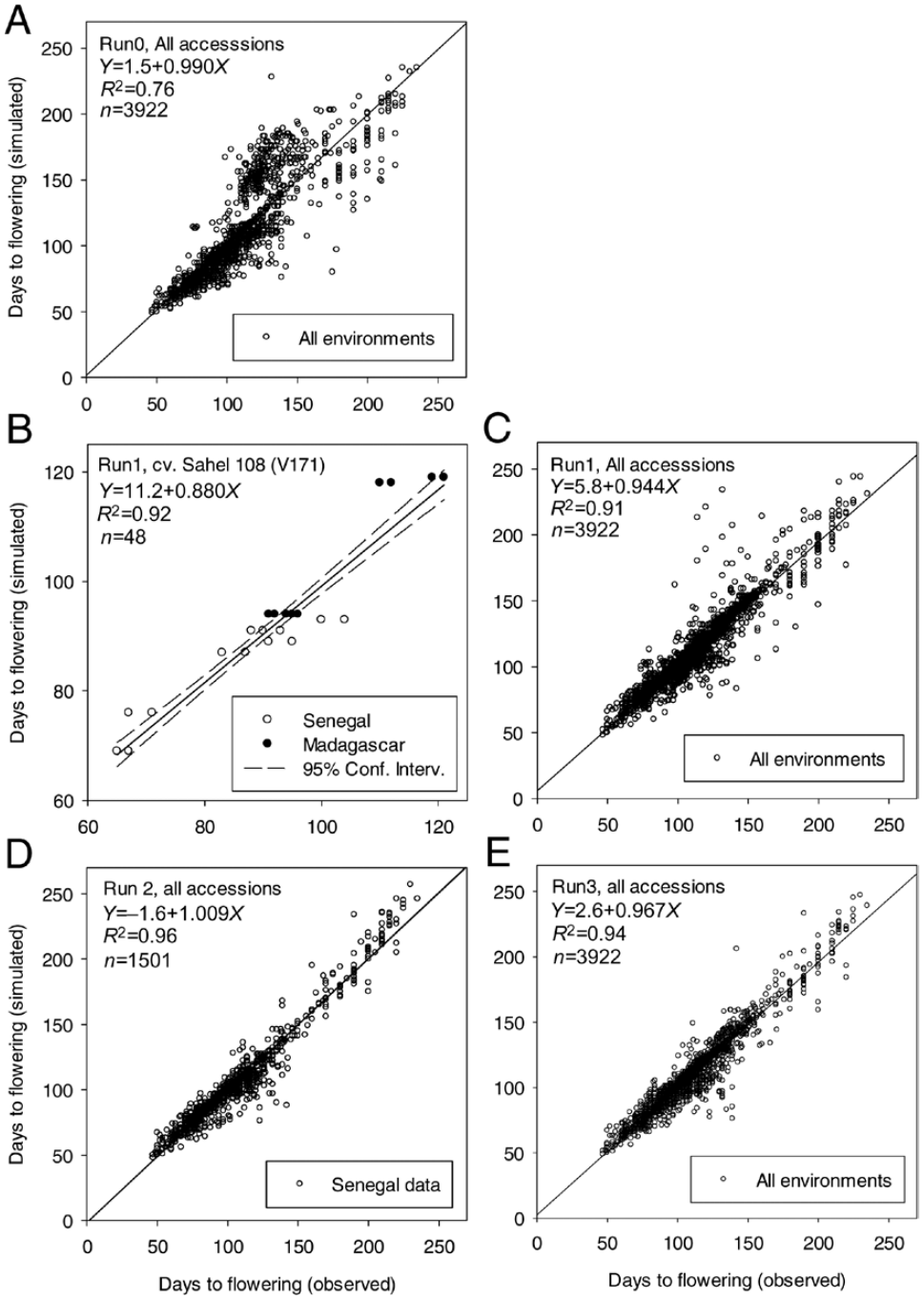

Fig. 4. Correlations of simulated *vs* observed time to flowering using estimated RIDEV parameters. (A) all accessions, estimation Run0; (B) check cv. Sahel 108, Run1; (C) all accessions, Run1; (D) all accessions, Run2 (Senegal data only); (E) all accessions, Run3. Estimation runs are explained in Table 2.

associations with $P=2.5 \times 10^{-9}$ *vs* 2.5×10^{-6} on chr6 and $P=1.0 \times 10^{-7}$ *vs* 7.9×10^{-6} on chr11. Six additional QTLs were detected for *1/PPsens* on chr1, 2, 3, 4, 9 and 11 (Fig. 5B and Table 3). The QTL *P9m* on chr9 ($P=2.0 \times 10^{-7}$) had two peak SNPs of equal *P* separated by 26 kb, which is within the estimated LD of 39 kb (Supplementary Fig. S5). The RIDEV parameter thus detected more and stronger QTLs than *PPindex*, but the two methods mostly yielded different QTLs. Parameters 1/*PPsens* and *PPindex* were correlated, although not strongly (1/*PPsens*=0.513 + 0.0184×*PPindex*; R^2=0.62).

Genomic associations for the duration of BVP

BVPindex yielded only weak associations having $P<1.0 \times 10^{-5}$ (Fig. 6A). The strongest was QTL *B6(1)i* and co-localized with *B6m* ($P=2.5 \times 10^{-6}$) for RIDEV parameter *BVPsum* (Fig. 6B: Run1). Two other weak associations for *BVPindex* co-localized with strong QTLs for RIDEV parameter *BVPmin* (Fig. 6C: *B2m′* with $P=7.9 \times 10^{-6}$ and *B6(2)m′* with $P=1.3 \times 10^{-7}$). A QTL on chr7 (*B7m*; $P=1.3 \times 10^{-6}$) was detected for *BVPsum* (Fig. 6B) but was not detected for *BVPindex*. Consequently, model

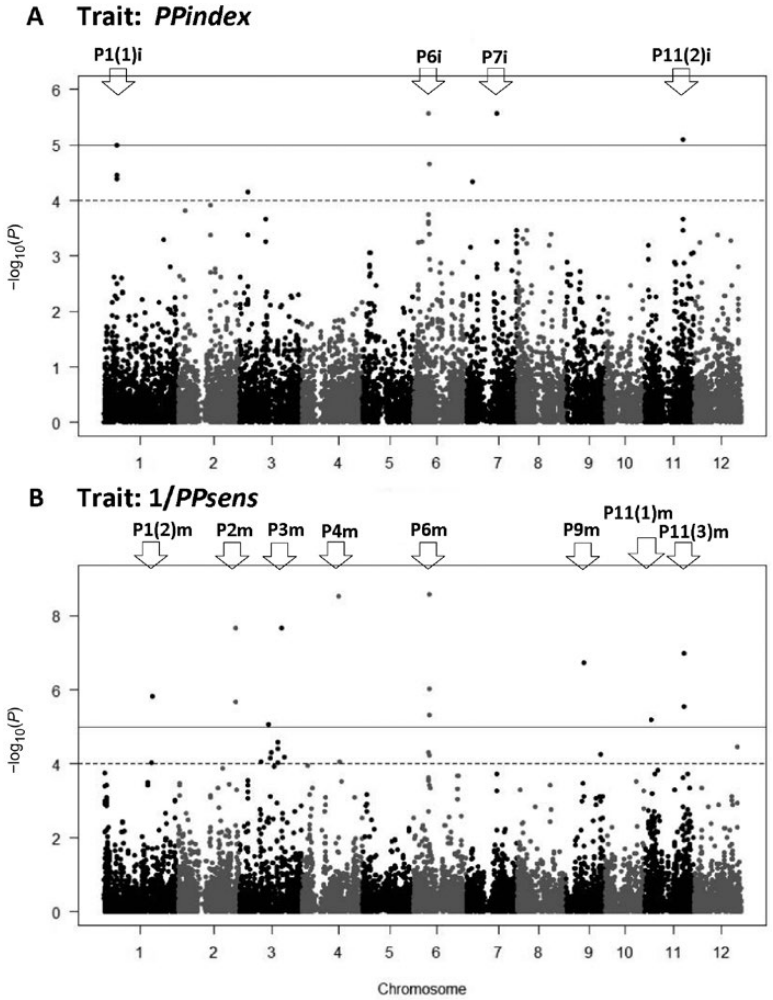

Fig. 5. Associations for photoperiod response. (A) index variable *PPindex*; (B) RIDEV model parameter 1/*PPsens* as estimated in Run1.

parameters informing on BVP gave more and stronger QTLs than *BVPindex*.

The QTLs reported for model parameters related to BVP were all obtained by estimation Run1 (Table 2). None were obtained with Run0. Consequently, the co-estimation of cardinal temperatures (Run1) was essential to detect QTLs for BVP-related model parameters.

Genomic associations for thermal response of duration to flowering

The *COLDIndex* calculated from duration to flowering for July (warm) and October (cold) sowings in Senegal gave a QTL on chr1 (Fig. 7A: *C1i*; $P=1.3 \times 10^{-5}$). The functionally comparable RIDEV *Tbase* parameter derived from the same phenomics dataset (Run2: Senegal environments only), which conveys thermal effects on flowering, did not replicate *C1i* but gave a larger QTL on chr6 (Fig. 7B: *C6m*; $P=2.0 \times 10^{-7}$). The same locus gave a much weaker association ($P=6.3 \times 10^{-5}$) for *COLDIndex* (compare Fig. 7A *vs* 7B).

The RIDEV Run3 (Table 2) across all environments and with the inclusion of *AcclimTb* gave a strong QTL ($P=2.5 \times 10^{-6}$) on chr1 (*H1m*; Fig. 7C). This QTL did not co-localize with any other QTL, although it was physically close to *C1i* (1.3 Mb).

Another index variable also related to temperature (*ALTIndex*) was calculated as the difference in duration to flowering between July sowing in Senegal (warm) and the high-altitude site in Madagascar (cold), with day length effects expected to be negligible. *ALTIndex* gave nine significant associations (Fig. 8A). Assuming that *ALTIndex* conveys thermal effects, we compared QTLs for *ALTIndex* and cardinal temperatures (Fig. 8B, C), estimated for Madagascar and Senegal environments combined (Run1). Only one QTL was detected for *Tbase* on chr1, *T1m* ($P=1.6 \times 10^{-5}$; Fig. 8B), which co-localized with *T1i* (Fig. 8A). The QTL *C6m* previously detected for *Tbase* for Senegal environments alone (Fig. 7B) was not observed.

For *Topt*, two strong associations were detected on chr8 and 9 (*T8(2)m* and *T9m*). Two weak associations ($P=3.2 \times 10^{-5}$) on chr3 and chr5 for *Topt* that visually co-localized with *T3(2)i* and *T5i* for *ALTindex* (Fig. 8C *vs* 8A) were actually different, with about 200 kb separating them. Consequently, the numerous associations detected for *ALTIndex* could not be explained with RIDEV parameters.

Annotated genes within QTLs

In Table 3, details of QTL parameters and putative candidate genes within ±100 kb and ±39 kb (±LD) of the peak SNP

Table 3. *Major QTLs having P<1×10^{-5}, at least three supporting SNPs with P<1 × 10^{-3} within LD region, and a frequency of at least 4% for the rarer allele*

Annotated genes located within ±100 kB of main SNP are listed with putative function. Distance of center of gene from SNP is provided as ×kB. Genes within the estimated LD of 39 kB of SNP are shown in bold. QTL ID, given code; Chr, chromosome number; Type, index variable or model parameter; Run, model parameter estimation run as in Table 2; Supp. SNPs, number of supporting SNPs having *P*<1.0 × 10^{-3}; Fig, figure showing the QTL graphically. A complete list of all QTLs having *P*<1 × 10^{-4} is presented in Supplementary Table S3. All QTLs carrying the same name but differ in suffix 'm' or 'I' (for model or index) colocalize within ±LD.

QTL ID	Chr	Trait	Type	Run	Locus of peak SNP (bp)	*P*	Supp. SNPs	Effect	Alleles		Allele frequency (no. acc.)		Genes	Fig	Putative candidate genes [distance from SNP in kbp], function
Traits for photoperiod effect on time of flowering															
P6i	6	*PPindex*	Index		9138014	2.51E–06	13	–27.2	G	T	156	38	25	5A	**Loc_Os06g16070 [11]**, serine/threonine kinase
P7i	7	*PPindex*	Index		17811153	2.51E–06	9	–31.7	A	T	175	19	20	5A	**Loc_Os07g30160 [8]**, syn. *TPP10*, trehalose phosphatase or T6P synthase, expressed in pollen; **Loc_Os07g30130 [32]**, MYB-like DNA binding domain; Loc_Os07g30250 [73], RFT1 family protein, flowering under long day
P11(2)i	11	*PPindex*	Index		22650475	7.94E–06	7	–20.2	A	T	119	75	30	5A	**Loc_Os11g38270 [14]**, syn. *OsFON2*, floral meristem size
P4m	4	*1/PPsens*	RIDEV	1	21450464	3.16E–09	8	–1.5	C	T	181	7	21	5B	Loc_Os04g35180 [72], heat shock protein; **Loc_Os04g35240 [33]**, serine/threonine kinase; **Loc_Os04g35270 [2]**, fucosyl tranf., neutral invertase
P6m	6	*1/PPsens*	RIDEV	1	9635471	2.51E–09	19	–0.98	A	T	166	22	12	5B	Loc_Os06g16660 to Loc_Os06g16720, retrotransposons expressed SNP located in transposon, gene-poor region
P9m	9	*1/PPsens*	RIDEV	1	10498775 10524485	2.00E–07	8	–1.6	A	T	181	7	22	5B	Gene-poor region (13 transposons, 3 Fbox proteins)
P11(1)m	11	*1/PPsens*	RIDEV	1	4240572	6.31E–06	4	–0.8	G	A	169	19	20	5B	Loc_Os11g08210 [60], syn. *OsNAC5*, ABA-dependent TF, apical meristem, flower morphogenesis, cold/salt tol.; **Loc_Os11g08080 [15]**, MYB-like DNA binding domain
P11(3)m	11	*1/PPsens*	RIDEV	01	23359728	1.00E–07	6	–1.4	G	A	179	9	25	5B	Loc_Os11g39160 [50], **Loc_Os11g39190 [24]**, **Loc_Os11g39260 [18]**, **Loc_Os11g39280 [31]**, **Loc_Os11g39290 [36]**, Loc_Os11g39310 [46], Loc_Os11g39320 [51], Loc_Os11g39330 [57], apoptotic ATPases; Loc_Os11g39370 [74], syn. *OsSERL1*, brassinosteroid sensitivity, serine/threonine kinase

Table 3. *Continued*

QTL ID	Chr	Trait	Type	Run	Locus of peak SNP (bp)	*P*	Supp. SNPs	Effect	Alleles		Allele frequency (no. acc.)		Genes	Fig	Putative candidate genes [distance from SNP in kbp], function
Traits for constitutive earliness of flowering															
B6m	6	*BVPsum*	RIDEV	1	25501329	2.51E–06	12	–423	T	C	170	18	19	6B	Gene-poor region (9 transposons, expressed)
B7m	7	*BVPsum*	RIDEV	1	23534067	1.26E–06	9	–635	T	A	181	7	25	6B	Loc_Os07g39220 [49], syn. *OsBZR1*, dwarfism/leaf angle; **Loc_Os07g39310 [8]**, serine/threonine kinase
Traits for thermal effects on time to flowering															
C6m	6	*Tbase*	RIDEV	2	2940078	2.00E–07	9	4.46	T	G	67	128	28	7B	**Loc_Os06g06300 [12]**, syn. *OsFTL3*, syn. *RFT1*, florigen, flowering time under long day; **Loc_Os06g06320 [1]**, syn. *HD3a*, syn. *OsFTL2*, flowering time under short day; SNP is within HD3a; **Loc_Os06g06380 [36]**/ Loc_Os06g06390 [42]/Loc_ Os06g06400 [48], apoptotic ATPases
T1i	1	*AltIndex*	Index		1358915	1.58E–05	10	–19.5	A	C	156	30	32	8A	Loc_Os01g03510 [58], stress protein, dwarfism; **Loc_Os01g03370 [0]**, serine/ threonine kinase
T5i	5	*AltIndex*	Index		930202	3.16E–06	6	–23.8	G	A	179	7	32	8A	Loc_Os05g02500 [70], syn. *OsMKP1*, dwarfism, gibberellin and brassinosteroid sensitivity, serine/threonine kinase; Loc_ Os05g02530 [51], photosynthetic capacity, root development, culm length, grain number; **Loc_Os05g02670 [14]**, microtubule motor activity, kinesin
T8(1)i	8	*AltIndex*	Index		2014082	5.01E–07	6	–27.9	A	T	160	26	26	8A	**Loc_Os08g04150 [0]**, RNA polymerase KOG1510; Loc_Os08g04210 [41]/Loc_ Os08g04230 [47]/Loc_Os08g04240 [50]/Loc_Os08g04250 [53], salt stress; Loc_Os08g04270 [66], grain size/filling/ dormancy, root branching
T8(2)m	8	*Topt*	RIDEV	1	10041544	7.94E–07	4	3.36	A	T	147	41	18	8C	**Loc_Os08g16430 [11]**, phytochrome P450-like; **Loc_Os08g16460 [38]**, apoptotic ATPase, up-regulated under cold stress in anthers

Table 3. *Continued*

QTL ID	Chr	Trait	Type	Run	Locus of peak SNP (bp)	*P*	Supp. SNPs	Effect	Alleles		Allele frequency (no. acc.)		Genes	Fig	Putative candidate genes [distance from SNP in kbp], function
T9m	9	*Topt*	RIDEV	1	20330067	3.98E–07	3	5.65	A	C	175	13	24	8C	Loc_Os09g34320 [71], methyl transferase; **Loc_Os09g34880 [2]**, seq.-specific DNA-binding TF, expressed in seed; **Loc_Os09g34950 [34]**, serine/threonine kinase; Loc_Os09g35000 [62], microspore development, flap endonuclease expressed in sperm cell under cold stress; Loc_Os09g35010 [66], syn. *DREB1*, drought/cold/salinity; Loc_Os09g35030 [74], syn. *DREB1A*, cold/drought/salinity tolerance
H1m	1	*AcclimTb*	RIDEV	3	43068623	2.51E–06	6		A	G	180	8	35	7C	Loc_Os01g74190 [90], radical SAM enzyme; **Loc_Os01g74410 [29]**, syn. *OsMYB59*, TF; Loc_Os01g74440 [44], syn. *OsMADS79*, MADS box transcription regulator; Loc_Os01g74520 [93], methyl transferase
					43072052	2.51E–06			A	G			32		Loc_Os01g74190 [94], radical SAM enzyme; **Loc_Os01g74410 [25]**, syn. *OsMYB59*, TF; Loc_Os01g74440 [41], syn. *OsMADS79*, MADS box transcription regulator; Loc_Os01g74520 [89], methyl transferase
					43123957	2.51E–06			A	G			36		Loc_Os01g74590 [71], MYB-TF; **Loc_Os01g74410 [27]**, syn. *OsMYB59*, TF; **Loc_Os01g74440 [11]**, syn. *OsMADS79*, MADS box transcription regulator; **Loc_Os01g74520 [37]**, methyl transferase
					43158965	2.51E–06			A	T			36		**Loc_Os01g74590 [35]**, MYB-TF; Loc_Os01g74410 [62], syn. *OsMYB59*, TF; Loc_Os01g74440 [46], syn. *OsMADS79*, MADS box transcription regulator; **Loc_Os01g74520 [2]**, methyl transferase
					43269458	2.51E–06			A	T			16		Loc_Os01g74590 [75], MYB-TF

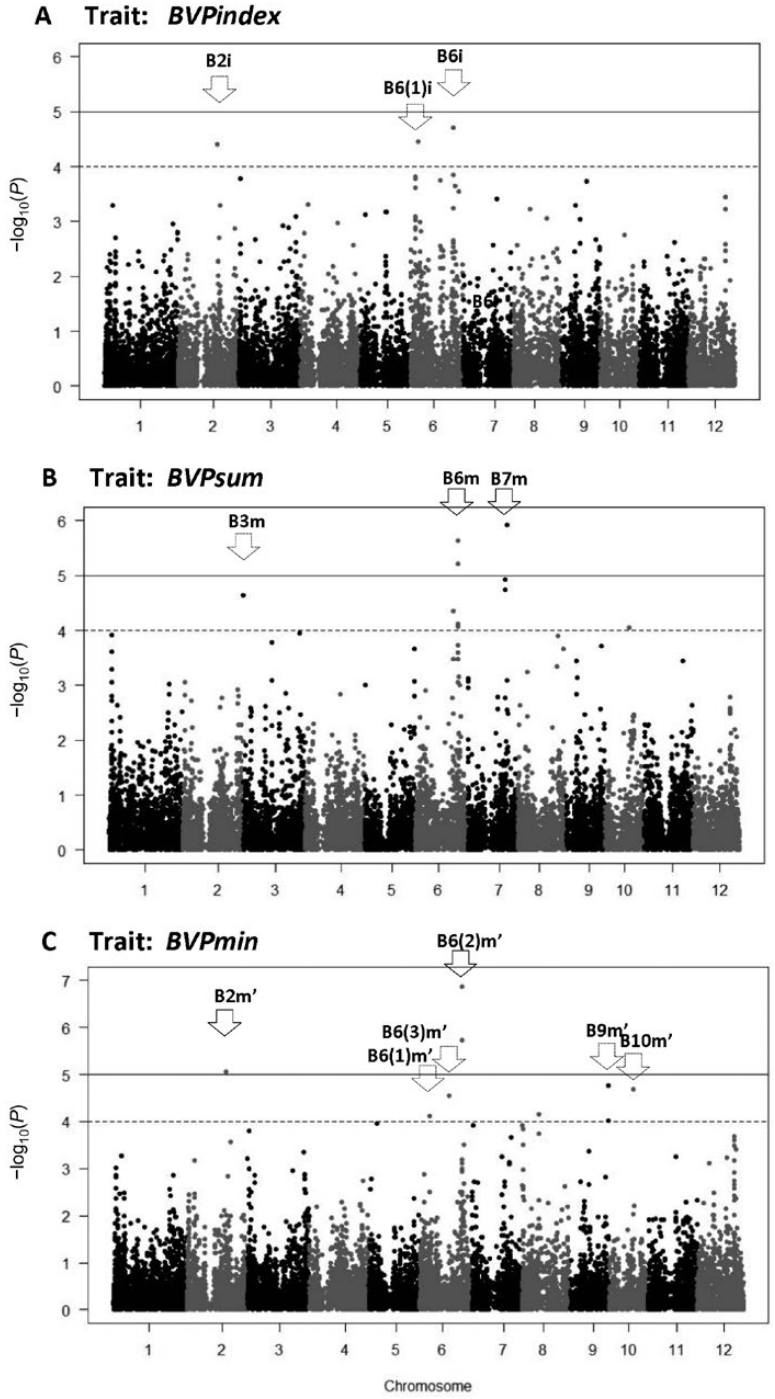

Fig. 6. Associations for basic vegetative phase duration. (A) *BVPindex*; (B) RIDEV parameter *BVPsum*; (C) RIDEV parameter *BVPmin*. RIDEV parameter estimation Run1.

are presented for the 18 QTLs that had $P<1 \times 10^{-5}$, ≥3 supporting SNPs and an allelic frequency of ≥4% for the minor allele (henceforth called major QTLs). Information on all 37 observed QTLs is presented in Supplementary Table S3. Within 100 kb, 12–37 genes were found. In some major QTLs, few functional genes occurred due to an abundance of transposons (e.g. *P9m*, *P6m* and *B6m*).

Genes known to participate in networks controlling flowering

A particularly interesting pair of candidate genes was associated with *C6m* (major QTL for *Tbase;* Fig. 7B; $P=2.0 \times 10^{-7}$). They were Loc_Os06g06300, syn. *OsFTL3*, syn. *RFT1*, a florigen promoting flowering under long days; and Loc_Os06g06320, syn. *HD3a*, syn. *OsFTL2*, a florigen promoting flowering under short days. The main SNP was located within *HD3a*.

Major QTL *P11(2)i* (*PPindex)* was associated with *OsFON2* (Loc_Os11g38270) controlling floral meristem size. The RFT1-family florigene Loc_Os07g30250 was found in QTL *P7i*. RIDEV parameter 1/*PPsens* did not pick up this locus but gave major QTL *P11(1)m* in which *OsNAC5* (Loc_Os11g08210) was detected, controlling floral morphogenesis. On major QTL *T8(2)m* (*Topt*), Loc_Os08g16430 was found, a gene associated with phytochrome P450.

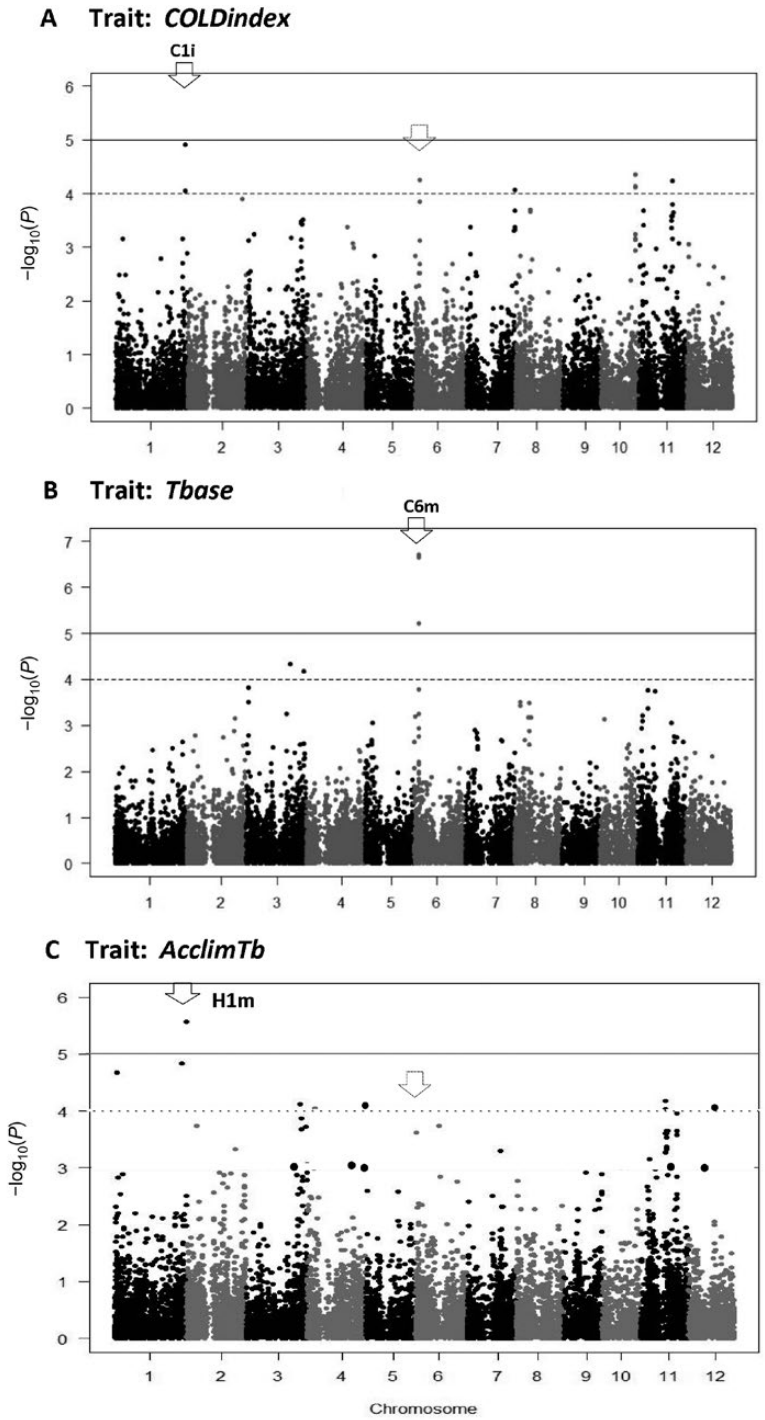

Fig. 7. Associations for low-temperature-related traits. (A) *COLDindex* (based on Senegal observations only); (B) RIDEV parameter *Tbase* estimated in Run2 (Senegal observations only); (C) RIDEV parameter *AcclimTb* estimated in Run3 (Senegal and Madagascar data combined). Unnamed dotted arrows indicate co-localizations with QTL *C6m*. For *AcclimTb* only the prominent QTL *H1m* was analysed (Table 3).

RIDEV parameters were associated with three MADS box genes [*OsMADS75* and *OsMADS76* in minor QTL *B6(3)m´* (*BVPmin*); *OsMADS79* in major QTL *H1m* (*AcclimTb*)]. Also associated with *BVPmin* was the day length-independent flowering gene *RID1* (Loc_Os10g28330 on minor QTL *B10m´*).

Other genes associated with development

Several candidate genes were related to dwarfism, although the well-known semidwarf gene *SD1* was not among them. Examples for major QTLs were *B7m* (Loc_Os07g39220 or *OsBZR1*, controlling dwarfism and leaf angle via brassinosteroid), *T1i* (Loc_Os01g03510, dwarfism) and *T5i* (Loc_Os05g02500, syn. *OsMKP1*, dwarfism, and gibberellin and brassinosteroid sensitivity; Loc_Os05g02530, photosynthetic capacity, root development, and culm length and grain number). This was also true for minor QTLs *P1(2)m* (Loc_Os01g49000, dwarfism and microtubule organization) and *T1m* (Loc_Os01g03510, dwarfism). Candidate genes related to developmental biology but not dwarfism

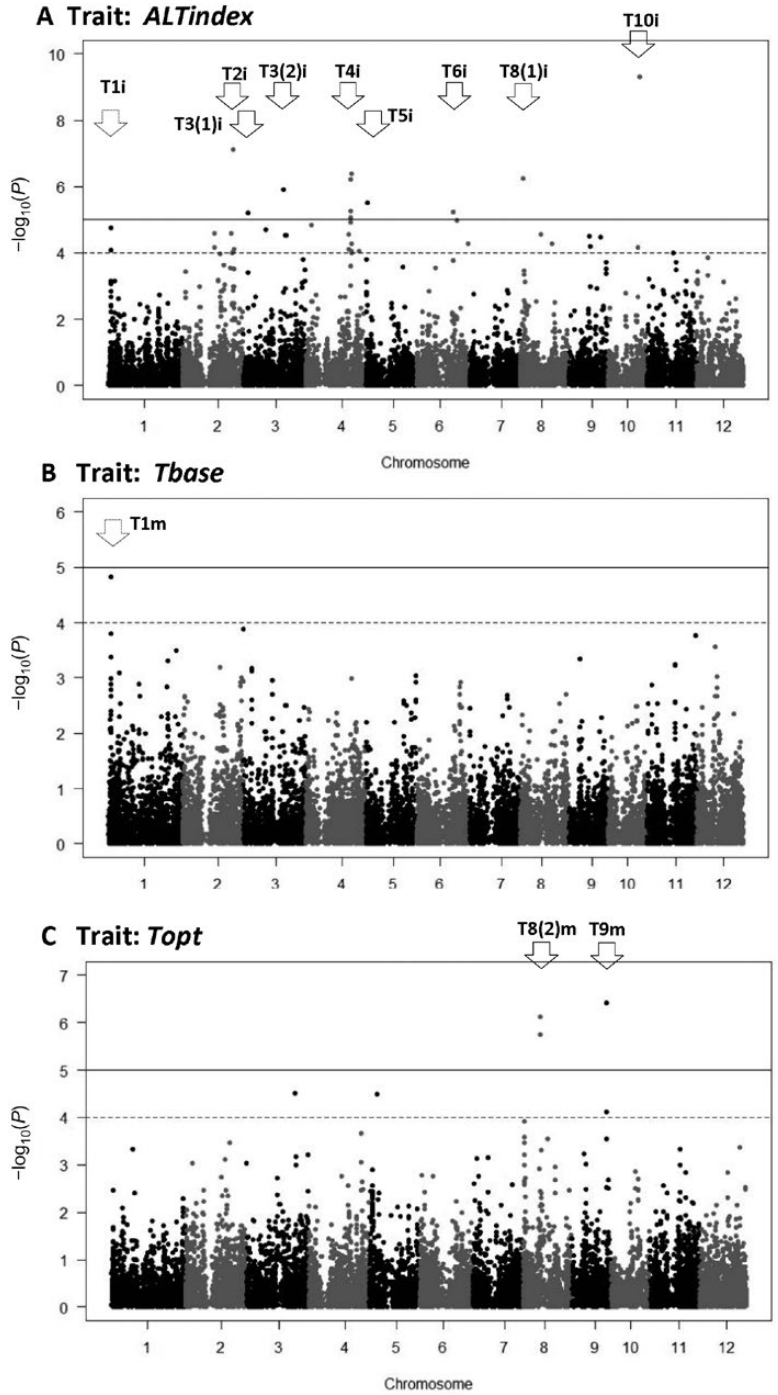

Fig. 8. Associations for temperature response traits (Senegal and Madagascar data combined). (A) *ALTIndex*; (B) RIDEV parameter *Tbase* estimated in Run1; (C) RIDEV parameter *Topt* estimated in Run 1.

were observed in major QTLs *T8(1)i* (Loc_Os08g04270; grain size/filling/dormancy, root branching) and *T9m* (Loc_Os09g35000, microspore development). Among the two candidate genes associated with trehalose-6-phosphate (T6P), a regulator of cell sink activity, Loc_Os07g30160 in QTL *P7i* (syn. *TPP10*) may be of interest because it is located near the center of the QTL and has known expression in pollen.

Phytohormone or stress related genes

Major QTLs having candidate genes known for abiotic stress responses were *T8(1)i* (Loc_Os08g04210, -230, -240, -250, salt stress) and *T9m* (Loc_Os09g35010, syn. *DREB1*, drought/cold/salinity). The numerous candidates related to phytohormones (auxin, gibberellin, ethylene, but not ABA), to oxidative stress, proline synthesis, heat-shock proteins, or fatty acid desaturase (cold adaptation) were associated with minor QTLs (Supplementary Table S3).

Putatively stress-related signaling function can also be attributed to serine/threonine kinases, which were found in ten QTLs. In two cases, the peak SNP was located within the gene [Loc_Os01g03370 in major QTL *T1i* (*ALTindex*), colocalized with minor QTL *T1m* (*Tbase*)]. The sole major

QTL associated with cold acclimation (*H1m*) had five SNPs of equal *P*-value, located in a genomic region that occurred on chr1 as five near-identical repeats. These regions contained several genes involved in transcription regulation and, putatively, epigenetic processes. The genes were Loc_Os01g74410 (MYB family TF), Loc_Os01g74440, syn. *OsMADS79* (MADS box transcription regulator), and Loc_Os01g74520 (methyl transferase). Putative genes controlling epigenetics were also seen in a minor QTL *B9m´* (Loc_Os09g39420, syn. *OsWD40-174*, histone transcription regulator; and Loc_Os09g39490, syn. *OsNFYB12*, histone-like TF).

Distribution of G and T alleles of QTL C6m *among accessions*

For the peak SNP on the *C6m* QTL, which was located within HD3a florigen (Table 3), we determined the distribution of G *vs* T alleles among accessions and phenotypes. The more abundant allele (G, 66%) was associated with lower *Tbase* (less cold sensitive), but also with high 1/*PPsens* (photoperiod sensitive), as shown in Table 4. The G-allele accessions had smaller *COLDindex* and their duration to flowering was less sensitive to high-altitude conditions, indicating smaller sensitivity to cool conditions.

In terms of genetic composition of the G- and T-groups, the molecular subgroups I1 and I3 (Dingkuhn *et al.*, 2015*a*) were nearly exclusively composed of G-types (>90%), whereas I2 group was predominantly T-type and the three aus-type accessions (I4) were also T-type. The G type was more abundant in traditional (84%) *vs* improved (46%) accessions but nearly absent in upland-adapted accessions (6%). It was frequent in Madagascar (91%), Nepal and Bhutan (91%), Bangladesh (100%) and Indochina (93%) accessions but less frequent in S. Asian, S. E. Asian, Indian and W. African accessions. Breeding products of IRRI and AfricaRice (52% and 23%) had different frequencies of the G allele. Details are presented in Supplementary Table S4.

Discussion

RIDEV model explains phenology variation among diverse environments

A previous version of RIDEV was used to explain multi-environment variation of rice phenology (Dingkuhn *et al.*, 1995) and genotypic differences (Dingkuhn and Miezan, 1995). The present RIDEV V2 incorporated recent findings on crop-generated microclimate (Julia and Dingkuhn, 2012, 2013) and day length control of flowering (Dingkuhn *et al.*, 2008). The model explained 96% of variation in time to flowering for the Senegal environments alone (Run2) but only 91% for Senegal and Madagascar environments combined (Run1). The fact that the cold-acclimation hypothesis (Run 3) reigned in most of the apparent outliers (R^2=0.94) indicates that some accessions showed adaptation when continuously exposed to low temperatures at high altitude. Cold acclimation has been reported for rice in terms of reduced spikelet sterility (Shimono *et al.*, 2010) but not for phenology. However, Shi *et al.* (2015) reported evidence for epigenetic control of flowering in rice.

Phenological acclimation to low temperatures, according to the concept of thermal time, would reduce either *Tbase* or the number of heat units (*BVPsum* in RIDEV), in both cases advancing flowering. Our choice of having acclimation act on *Tbase* was arbitrary and would require dedicated experiments to validate. Zhang *et al.* (2008) reported an apparent increase in heat units needed by rice varieties to flower as climate warmed over a period of 20 years. In fact, they observed constant duration to flowering despite the warming. Similarly, in our study, cool conditions increased duration to flowering less when they were a permanent condition (high altitude). We tested alternative factors such as atmospheric humidity but retained cold acclimation because it explained phenological variation best. Full validation of this hypothesis will require controlled environment studies.

RIDEV parameters are biologically meaningful—but what do they mean?

Duration to flowering is prone to genotype × environment interactions (G×E). Some G×E have a known physiological basis, such as day length and thermal control of development (Dingkuhn *et al.*, 1995, 2015*b*). The modelling concepts of genotypic thermal-time budgets, cardinal temperatures and photoperiod sensitivity were implemented in RIDEV to heuristically extract G effects while factoring in E effects. Adding cold acclimation gave excellent phenotype predictability (R^2=0.94). However, this in itself is no proof of biological model accuracy. In fact, there is no obvious similarity between the complex gene networks controlling flowering in rice (Shrestha *et al.*, 2014) and physiological concepts such as genotypic thermal-time budgets. Yin *et al.* (2005), however, demonstrated for barley that such model parameters are associated with specific genomic loci, and conversely, QTL

Table 4. *Mean trait values observed for accessions carrying G or T allele on QTL* C6m

Parameter	Accession with G-allele (mean±SE)	Accession with T-allele (mean±SE)
Tbase [°C], RIDEV	8.15 ± 0.36	12.67 ± 0.25
1/PPsens [unitless], RIDEV	1.67 ± 0.11	0.86 ± 0.02
BVPmin [d], RIDEV	44.4 ± 0.9	36.9 ± 1.1
COLDindex, Senegal [unitless]	1.30 ± 0.01	1.42 ± 0.02
Delta-duration, high/mid alt., Madagascar [d]	18.5 ± 1.6	23.7 ± 0.7

effects when built into the model can predict flowering time. For rice, Nakagawa *et al.* (2005) dissected traits with a statistical model predicting flowering of a bi-parental population, yielding QTLs for the known heading-date loci *Hd1*, *Hd2*, *Hd6* and *Hd8*. Consequently, even if the phenology model simplifies biological processes and forces *ex ante* theory upon the data, it can meaningfully link physiology to genomics. The limitations, apart from model accuracy, are G variation (associations can only be detected if polymorphisms are present) and E variation (E effects occur only when experimentally challenged). Biparental populations and controlled environments thus limit discovery potential at G and E levels, respectively.

The present study extended the approaches of Nakagawa *et al.* (2005) and Yin *et al.* (2005) by using a diversity panel and exposing it to climate variation caused by latitude, altitude and season under field conditions. Greater scope for discovery was associated with greater challenge to the model's skills as E and G were more complex. We did find that the original model was insufficient and had to introduce an acclimation parameter to improve phenotype prediction.

We used two criteria for the meaningfulness of the RIDEV parameters, (i) phenotype variation explained and (ii) quality of genomic associations obtained. The former ascertained that phenotype and environment variation were maximally linked in the analysis. The latter, when associated with known QTLs or genes having a function related to the trait, suggested that the parameters had biological meaning. The index variables calculated from the same datasets (*PPindex*, *COLDindex*, *ALTindex*, *BVPindex*; Dingkuhn *et al.*, 2015*b*) served as backdrop for model performance. RIDEV parameters mostly gave more and stronger QTLs than index variables, although rarely the same. This means that RIDEV increased analytical power and its parameters were biologically meaningful, but they did not exactly describe the same traits as those described by the index variables. Only the function of the causative genes underlying the QTLs, once analysed, can inform *a posteriori* on the exact biological meaning of the parameters.

The inevitable interactions among crop parameters describing different processes but contributing to the same outcome (flowering) are a problem that can only be overcome by choosing environments that differentiate among individual parameter effects. Sensitivity analysis indicated distinct effects among *PPsens*, and *AcclimTb* and the group of three thermal budget parameters (*Tbase*, *Topt* and *BVPsum*), which had similar effects and thus may cause over-parameterization. However, the absence of any QTLs for *BVPsum* for the 'minimalist' Run0 (estimation of only *BVPsum* and *PPsens*) indicated that the co-estimation of cardinal temperatures was necessary to obtain associations for thermal-budget traits. We also ran GWAS for their aggregate derivative, *BVPmin*. However, *Tbase*, *Topt* and *BVPsum* gave more and different QTLs compared with *BVPmin*, indicating that their behavior was distinct.

Many candidate genes with plausible function

With 10–20 annotated genes present within the LD per association, and detailed haplotype information unavailable, candidate gene search relied on reported function and stage/organ specificity of expression using public databases.

Florigens and genes controlling shoot development

The association of *Tbase* with a highly significant SNP located inside the *HD3a* florigen (major QTL *C6m*) is an important finding. This SNP is potentially causative. *HD3a* and its immediate neighbor, the florigen *RFT1*, stand at the bottom of a complex cascade of at least 19 genes controlling flowering in rice, not counting circadian clock genes that control several genes of this network (Shrestha *et al.*, 2014). HD3a promotes flowering under short days and RFT1 under long days. Gómez-Ariza *et al.* (2015) reported that genotypes flowering early in temperate (cool) climates express HD3a even under long days, which is characteristic of rice varieties selected for Europe. *HD3a* is thus a key gene for earliness under cool conditions. Fittingly, *Tbase* affects time to flowering in a temperature-dependent but day length-independent manner (Dingkuhn and Miezan, 1995).

The minor G-allele for low *Tbase* was frequent (33%) and its distribution interesting. Its greater abundance in accessions from Madagascar, Nepal, Bhutan and Bangladesh (which has a cool Boro rice season), and in the cold-tolerant I3 genetic group (Dingkuhn *et al.*, 2015*a*), points at a climate-related selection history for the allele. Accessions carrying G allele had lower *Tbase* and their crop duration was less affected by altitude (Madagascar) and the cool season (Senegal; *COLDindex*), while *BVPmin* differed little between the alleles. However, G accessions were on average more photoperiod sensitive. This could be caused by genetic linkage (neighborhood of *HD3a* and *RFT1*, the latter promoting flowering under LD) or physiological linkages. The G allele was frequent in photoperiod-insensitive, improved accessions from S. E. Asia. Its frequent occurrence in photoperiod sensitivity accessions may thus not be causal but a result of co-selection.

Another flowering gene, *RID1*, syn. *EHD2*, was associated with RIDEV parameter *BVPmin*. *EHD2* controls both *HD3a* and *RFT1* through the central switch *EHD1*, which is under circadian control (Shrestha *et al.*, 2014). Dysfunction of *EHD2* causes late flowering and tallness (Hu *et al.*, 2013). *RIDEV* QTLs were also associated with MADS box genes (*OsMADS75*, *76*, and *79*), a family involved in developmental and flowering processes (Arora *et al.*, 2007). In contrast to the central importance of *OsMADS50*, *51*, and *56* (Shrestha *et al.*, 2014), the role in flowering of the genes found here is less known.

Flowering genes were also associated with day length response. For *PPindex* QTLs, *OsFON2* controlling floral meristem size (Suzaki *et al.*, 2006) and another *RFT1*-family gene (Loc_Os07g30250) conveying photoperiod sensitivity (Shrestha *et al.*, 2014) were identified. RIDEV parameter 1/*PPsens* did not pick up these genes but gave an association with *OsNAC5*, a stress tolerance gene (Takasaki *et al.*, 2010; Jeong *et al.*, 2013) that is also known to control flower morphogenesis (http://shigen.nig.ac.jp/rice/oryzabase/gene/detail/2047).

Only one of the many heading date (HD) QTLs described in the literature was identified here by GWAS, whereas

Nakagawa *et al.* (2005) obtained several HD QTLs with the help of a phenology model. That study, however, used a wide cross (*indica vs* temperate *japonica*) involving polymorphisms in these highly conserved genes. Within the *indica* subspecies, a different spectrum of polymorphisms can be expected.

The observed association with *PPindex* of *TPP10*, a trehalose phosphatase playing a pivotal role in sink regulation by controlling T6P sugar signaling, may be surprising. However, Wahl *et al.* (2013) reported recently that T6P has an important role in flowering control.

Thermal adaptation and acclimation

Many QTLs had genes not known for flowering *per se* but thermal adaptation. Although all traits were derived from flowering date, the thermal extremes in Senegal and Madagascar expressed such adaptations, captured by *Tbase*, *Topt* and *AcclimTb*. Stress genes *DREB1* and *DREB1A* (Ito *et al.*, 2006; Mao and Chen, 2012) were associated with *Topt*, as was the apoptotic ATPase Loc_Os08g16460, which is strongly up-regulated in anthers under cold stress (Bai *et al.*, 2015), and the cold-responsive endonuclease Loc_Os09g35000, involved in microspore development. The transcription factor *OsMYB59* (syn. *OsMYB48-1*; Baldoni *et al.*, 2015) associated with *AcclimTb* is an important stress response gene (Park *et al.*, 2010; Xiong *et al.*, 2014) and regulatory hub (Smita *et al.*, 2015). Loc_Os03g01320 associated with minor QTL *B3m* was reported to participate in rice heat response (Mellacheruvu *et al.*, 2016). More generally, the abundance of NAC-type stress-responsive genes (Fang *et al.*, 2008, Park *et al.*, 2010, Nuruzzaman *et al.*, 2013), oxidative stress-related genes and serine/threonine kinases (Kulik *et al.*, 2011) in QTL regions also suggests that thermal stress was an important factor in the variation of flowering time.

Acclimation is an important component of thermal adaptation (Shimono *et al.*, 2010; Koumoto *et al.*, 2014). When epigenetically controlled it is conveyed by DNA-, RNA- or histone-modifying genes (Chinnusamy and Zhu, 2009). Several of our candidate genes reportedly convey epigenetic control, such as the *OsMADS* genes already mentioned (Kapazoglou *et al.*, 2012) and *OsWD40-174*, a HIRA histone chaperon involved in knox silencing controlled by ABA-responsive miRNA (Liu *et al.*, 2009). Interestingly, the *H1m* major QTL for cold acclimation was associated with Loc_Os01g74520 (methyl transferase) and Loc_Os01g74190 (radical SAM enzyme; Fujimori, 2013), both being nucleic acid methylation genes putatively conveying epigenetic transcription control. Also within QTL *H1m* were Loc_Os01g74590 (MYB-family), *OsMYB59* (identical to *OsMYB48-1*), and *OsMADS79*, important regulatory hubs for transcription as described above. These putative cold-acclimation genes underlying QTL *H1m* occurred in a small, five-fold repeated region, associated with five equally significant SNPs. It thus appears likely that *AcclimTb* is associated with epigenetic processes.

The spectrum of genes associated with the QTLs suggests that phenological adaptation to the environments studied here involved a combination of developmental, thermal stress-related and epigenetic acclimation factors, in large part through transcription factors participating in gene networks controlling thermal sensing and response (Zhang and Tao, 2013). A conceptual conclusion from this finding is that although most crop models separate development control from physiological stresses, the ensemble of candidate genes reported here suggests stress response networks to be intimately connected with the control of flowering.

Conclusion

Overall, the types of genes located in the majority of QTLs reflected the nature of the traits investigated. All measured traits were related to development and flowering, and they involved either thermal or photoperiod responses. Many candidate genes were thus related to flowering control, dwarfism, cold or heat tolerance, and stress responses in general. Putatively epigenetic genes were specifically associated with the cold acclimation parameter of RIDEV. Which candidates were causative remains to be determined through haplotype analyses and experimental validation.

The larger number of major QTLs extracted with RIDEV across many environments, as opposed to the index variables derived from pairs of environments, provided proof of concept for model-assisted phenotyping for multi-environment field data. The present results may benefit molecular breeding upon validation of the QTLs. The most promising lead for crop improvement was QTL *C6m*. The hypothesis of the SNP located within *HD3a* being causative for low temperature adaptation merits further research.

Supplementary data

Supplementary data are available at *JXB* online.

Protocol S1. C++ code for RIDEV.

Fig. S1. Quantile–quantile (QQ) plots for GWAS.

Fig. S2. Correlations of calculated *vs* observed $T_{w(min)}$ and air–water T_{max} differentials.

Fig. S3. Sensitivity analysis of RIDEV simulations to variation of crop parameters.

Fig. S4. Frequency distributions of index variables.

Fig. S5. Decay of linkage as function of distance from significant SNPs.

Table S1. Detailed list of genotypes.

Table S2. RIDEV V2 parameters and input/output variables.

Table S3. List of all observed GWAS associations.

Table S4. Distribution of G/T alleles for QTL *C6m* by genetic subgroup, ecosystem and origin.

Acknowledgements

The authors would like to thank Drs Brigitte Courtois and Nourollah Ahmadi for valuable assistance in data analysis, as well as the excellent field staff of Africa Rice Center in Senegal and the Cirad-FOFIFA team in Madagascar.

References

Arora R, Agarwal P, Ray S, Singh AK, Singh VP, Tyagi AK, Kapoor S. 2007. MADS-box gene family in rice: genome-wide identification,

organization and expression profiling during reproductive development and stress. BMC Genomics **8,** 242.

Bai B, Wu J, Sheng WT, Zhou B, Zhou LJ, Zhuang W, Yao DP, Deng QY. 2015. Comparative analysis of anther transcriptome profiles of two different rice male sterile lines genotypes under cold stress. International Journal of Molecular Sciences **16,** 11398–11416.

Baldoni E, Genga A, Cominelli E. 2015. Plant MYB transcription factors: their role in drought response mechanisms. International Journal of Molecular Sciences **16,** 15811–15851.

Bradbury PJ, Zhang Z, Kroon DE, Casstevens TM, Ramdoss Y, Buckler ES. 2007. TASSEL: software for association mapping of complex traits in diverse samples. Bioinformatics **23,** 2633–2635.

Browning SR, Browning BL. 2007. Rapid and accurate haplotype phasing and missing-data inference for whole-genome association studies by use of localized haplotype clustering. American Journal of Human Genetics **81,** 1084–1097.

Chinnusamy V, Zhu JK. 2009. Epigenetic regulation of stress responses in plants. Current Opinion in Plant Biology **12,** 133–139.

Courtois B, Audebert A, Dardou A, *et al*. 2013. Genome-wide association mapping of root traits in a japonica rice panel. PLoS ONE **8,** e78037.

De Datta SK. 1981. Principles and practices of rice production. New York: John Wiley & Sons, 618.

Dingkuhn M. 1995. Climatic determinants of irrigated rice performance in the Sahel. III. Characterizing environments by simulating the crop's photothermal responses. Agricultural Systems **48,** 435–456.

Dingkuhn M. 1997. Characterizing irrigated rice environments using the rice phenology model RIDEV. In: Miezan KM, Wopereis MCS, Dingkuhn M, Deckers J, Randolph TF, eds. Irrigated rice in the sahel: prospects for sustainable development. Bouake, Cote d'Ivoire: West Africa Rice Development Association, 343–360.

Dingkuhn M, Kouressy M, Vaksmann M, Clerget B, Chantereau J. 2008. Applying to sorghum photoperiodism the concept of threshold-lowering during prolonged appetence. European Journal of Agronomy **28,** 74–89.

Dingkuhn M, Miezan KM. 1995. Climatic determinants of irrigated rice performance in the Sahel. II. Validation of photothermal constants and characterization of genotypes. Agricultural Systems **48,** 411–434.

Dingkuhn M, Radanielina T, Raboin L-M, *et al*. 2015*a*. Field phenomics for response of a rice diversity panel to ten environments in Senegal and Madagascar. 2. Chilling-induced spikelet sterility. Field Crops Research **183,** 282–293.

Dingkuhn M, Sow A, Manneh B, Radanielina T, Raboin L-M, Dusserre J, Ramatsoanirina A, Shreshta S, Ahmadi N, Courtois B. 2015*b*. Field phenomics for response of a rice diversity panel to ten environments in Senegal and Madagascar. 1. Plant phenological traits. Field Crops Research **183,** 342–355.

Dingkuhn M, Sow A, Samb A, Diack S, Asch F. 1995. Climatic determinants of irrigated rice performance in the Sahel. I. Photothermal and microclimatic responses of flowering. Agricultural Systems **48,** 385–410.

Fang Y, You J, Xie K, Xie W, Xiong L. 2008. Systematic sequence analysis and identification of tissue-specific or stress-responsive genes of NAC transcription factor family in rice. Molecular Genetics and Genomics **280,** 547–563.

Fujimori DG. 2013. Radical SAM-mediated methylation reactions. Current Opinion in Chemical Biology **17,** 597–604.

Fukai S. 1999. Phenology in rainfed lowland rice. Field Crops Research **64,** 51–60.

Gómez-Ariza J, Galbiati F, Goretti D, Brambilla V, Shrestha R, Pappolla A, Courtois B, Fornara F. 2015. Loss of floral repressor function adapts rice to higher latitudes in Europe. Journal of Experimental Botany **66,** 2027–2039.

Hammer GL, Kropff MJ, Sinclair TR, Porter JR. 2002. Future contributions of crop modelling: from heuristics and supporting decision making to understanding genetic regulation and aiding crop improvement. European Journal of Agronomy **18,** 15–31.

Hu S, Dong G, Xu J, *et al*. 2013. A point mutation in the zinc finger motif of RID1/EHD2/OsID1 protein leads to outstanding yield-related traits in japonica rice variety Wuyunjing 7. Rice **6,** 24.

Ito Y, Katsura K, Maruyama K, Taji T, Kobayashi M, Seki M, Shinozaki K, Yamaguchi-Shinozaki K. 2006. Functional analysis of rice DREB1/CBF-type transcription factors involved in cold-responsive gene expression in transgenic rice. Plant & Cell Physiology **47,** 141–153.

Jeong JS, Kim YS, Redillas MC, Jang G, Jung H, Bang SW, Choi YD, Ha SH, Reuzeau C, Kim JK. 2013. OsNAC5 overexpression enlarges root diameter in rice plants leading to enhanced drought tolerance and increased grain yield in the field. Plant Biotechnology Journal **11,** 101–114.

Julia C, Dingkuhn M. 2012. Variation in time of day of anthesis in rice in different climatic environments. European Journal of Agronomy **43,** 166–174.

Julia C, Dingkuhn M. 2013. Predicting temperature induced sterility of rice spikelets requires simulation of crop-generated microclimate. European Journal of Agronomy **49,** 50–60.

Kapazoglou A, Engineer C, Drosou V, Kalloniati C, Tani E, Tsaballa A, Kouri ED, Ganopoulos I, Flemetakis E, Tsaftaris AS. 2012. The study of two barley type I-like MADS-box genes as potential targets of epigenetic regulation during seed development. BMC Plant Biology **12,** 166.

Kawahara Y, de la Bastide M, Hamilton JP, *et al*. 2013. Improvement of the *Oryza sativa* Nipponbare reference genome using next generation sequence and optical map data. Rice **6,** 4.

Koumoto T, Shimakage R, Yokoi S, Shimono H. 2014. Memory over the generations: chilling tolerance at booting stage of next generation can be improved by abiotic stresses in rice. ASA, CSSA, SSSA International Annual Meeting, Long Beach, CA, Poster No. 513, https://scisoc.confex.com/scisoc/2014am/webprogram/Paper88805.html.

Kulik A, Wawer I, Krzywińska E, Bucholc M, Dobrowolska G. 2011. SnRK2 protein kinases—key regulators of plant response to abiotic stresses. OMICS **15,** 859–872.

Liu Q, Zhang YC, Wang CY, Luo YC, Huang QJ, Chen SY, Zhou H, Qu LH, Chen YQ. 2009. Expression analysis of phytohormone-regulated microRNAs in rice, implying their regulation roles in plant hormone signaling. FEBS Letters **583,** 723–728.

Mao D, Chen C. 2012. Colinearity and similar expression pattern of rice DREB1s reveal their functional conservation in the cold-responsive pathway. PLoS ONE **7,** e47275.

Mellacheruvu S, Tamirisa S, Vudem DR, Khareedu VR. 2016. Pigeonpea hybrid-proline-rich protein (CcHyPRP) confers biotic and abiotic stress tolerance in transgenic rice. Frontiers in Plant Science **6,** 1167.

Nakagawa H, Yamagishi J, Miyamoto N, Motoyama M, Yano M, Nemoto K. 2005. Flowering response of rice to photoperiod and temperature: a QTL analysis using a phenological model. Theoretical and Applied Genetics **110,** 778–786.

Nuruzzaman M, Sharoni AM, Kikuchi S. 2013. Roles of NAC transcription factors in the regulation of biotic and abiotic stress responses in plants. Frontiers in Microbiology **4,** 248.

Park MR, Yun KY, Mohanty B, Herath V, Xu F, Wijaya E, Bajic VB, Yun SJ, De Los Reyes BG. 2010. Supra-optimal expression of the cold-regulated OsMyb4 transcription factor in transgenic rice changes the complexity of transcriptional network with major effects on stress tolerance and panicle development. Plant, Cell & Environment **33,** 2209–2230.

Rebolledo MC, Dingkuhn M, Courtois B, Clément-Vidal A, Cruz DF, Duitama J, Lorieux M, Luquet D. 2015. Phenotypic and genetic dissection of component traits for early vigor in rice using plant growth modelling, sugar content analyses and association mapping. Journal of Experimental Botany **66,** 5555–5566.

Reicosky DC, Winkelman LJ, Baker JM, Baker DG. 1989. Accuracy of hourly air temperatures calculated from daily minima and maxima. Agricultural and Forest Meteorology **46,** 193–209.

Shi J, Dong A, Shen W-H. 2015. Epigenetic regulation of rice flowering and reproduction. Frontiers in Plant Science **5,** 803.

Shimono H, Ishii A, Kanda E, Suto M, Nagano K. 2010. Genotypic variation in rice cold tolerance responses during reproductive growth as a function of water temperature during vegetative growth. Crop Science **51,** 290–297.

Shrestha S, Asch F, Brueck H, Giese M, Dusserre J, Ramanantsoanirina A. 2013. Phenological responses of upland rice grown along an altitudinal gradient. Environmental and Experimental Botany **89,** 1–10.

Shrestha R, Gómez-Ariza J, Brambilla V, Fornara F. 2014. Molecular control of seasonal flowering in rice, arabidopsis and temperate cereals. Annals of Botany **114,** 1445–1458.

Smita S, Katiyar A, Chinnusamy V, Pandey DM, Bansal KC. 2015. Transcriptional regulatory network analysis of MYB transcription factor family genes in rice. Frontiers in Plant Science **6,** 1157.

Song Y, Gao Z, Luan W. 2012. Interaction between temperature and photoperiod in regulation of flowering time in rice. Science China. Life Sciences **55,** 241–249.

Suzaki T, Toriba T, Fujimoto M, Tsutsumi N, Kitano H, Hirano HY. 2006. Conservation and diversification of meristem maintenance mechanism in *Oryza sativa*: function of the FLORAL ORGAN NUMBER2 gene. Plant & Cell Physiology **47,** 1591–1602.

Sved JA. 1971. Linkage disequilibrium and homozygosity of chromosome segments in finite populations. Theoretical Population Biology **2,** 125–141.

Takasaki H, Maruyama K, Kidokoro S, Ito Y, Fujita Y, Shinozaki K, Yamaguchi-Shinozaki K, Nakashima K. 2010. The abiotic stress-responsive NAC-type transcription factor OsNAC5 regulates stress-inducible genes and stress tolerance in rice. Molecular Genetics and Genomics **284,** 173–183.

Wahl V, Ponnu J, Schlereth A, Arrivault S, Langenecker T, Franke A, Feil R, Lunn JE, Stitt M, Schmid M. 2013. Regulation of flowering by trehalose-6-phosphate signaling in *Arabidopsis thaliana*. Science **339,** 704–707.

Wopereis MCS, Haefele SM, Dingkuhn M, Sow A. 2003. Decision support tools for irrigated rice-based systems in the Sahel. In: Struif Bontkes TE, Wopereis MCS, eds. A practical guide to decision-support tools for agricultural productivity and soil fertility enhancement in sub-Saharan Africa. Wageningen, The Netherlands: IFDC and CTA, 114–126.

Xiong H, Li J, Liu P, Duan J, Zhao Y, Guo X, Li Y, Zhang H, Ali J, Li Z. 2014. Overexpression of OsMYB48-1, a novel MYB-related transcription factor, enhances drought and salinity tolerance in rice. PLoS ONE **9,** e92913.

Yin X, Struik PC, van Eeuwijk FA, Stam P, Tang J. 2005. QTL analysis and QTL-based prediction of flowering phenology in recombinant inbred lines of barley. Journal of Experimental Botany **56,** 967–976.

Zhang S, Tao F. 2013. Modeling the response of rice phenology to climate change and variability in different climatic zones: comparisons of five models. European Journal of Agronomy **45,** 165–176.

Zhang T, Zhu J, Yang X. 2008. Non-stationary thermal time accumulation reduces the predictability of climate change effects on agriculture. Agricultural and Forest Meteorology **148,** 1412–1418.